Journal of Inorganic Biochemistry 195 (2019) 130–140

Contents lists available at ScienceDirect

Journal of Inorganic Biochemistry

journal homepage: www.elsevier.com/locate/jinorgbio

Pt(IV) hybrids containing a TDO inhibitor serve as potential anticancer immunomodulators

Shixian Hua[a,1], Feihong Chen[a,b,1], Xinyi Wang[a], Yuanjiang Wang[a], Shaohua Gou[a,b,*]

[a] Pharmaceutical Research Center and School of Chemistry and Chemical Engineering, Southeast University, Nanjing 211189, China
[b] Jiangsu Province Hi-Tech Key Laboratory for Bio-medical Research, Southeast University, Nanjing 211189, China

ARTICLE INFO

Keywords:
Platinum(IV) hybrids
Tryptophan 2,3-dioxygenase
Antitumor
Immunomodulator
Immuno-chemotherapy

ABSTRACT

Tryptophan 2,3-dioxygenase (TDO), an immunosuppressive enzyme, can involve in immune evasion and tumor tolerance. TDO inhibitors can boost the efficacy of chemotherapeutics by promoting immunity. Herein, a strategy to introduce a TDO inhibitor into Pt(IV) complexes for reversing tumor immune suppression was adopted. A mono-modified Pt(IV) complex, 3, displayed significant antitumor activity against human liver cancer cells. Flow cytometry study revealed that complex **3** could induce cell death via a mitochondrial-dependent apoptosis pathway and arrest the cell cycle at S phase. Furthermore, complex **3** was effective to enhance T-cell immune responses by inhibiting the TDO enzyme expression to block the kynurenine production and inactivating the downstream of aryl hydrocarbon receptor (AHR).

1. Introduction

Recent developments have proved that immunotherapy is a highly effective strategy in treating cancer, which include cancer vaccines, chimeric antigen receptor (CAR) T-cell therapies, dendritic cell therapies and immune checkpoint inhibitors [1–3]. Immune checkpoint therapies, such as cytotoxic T-lymphocyte antigen (CTLA), T-cell immunoglobulin and mucin 3 domain (TIM3), programmed death-ligand 1 (PD-L1) and indoleamine 2,3-dioxygenase (IDO)/tryptophan 2,3-dioxygenase (TDO), are the most promising approaches, because they can act on the immunosuppression within the tumor microenvironment by protein expression levels and (or) biological functions, and regulate T cells to affect antitumor immune responses [1,4–6]. Hence, combination of immune checkpoint inhibitors with standard chemotherapeutic agents may be a promising strategy to improve the efficacy of cancer treatments.

Both IDO and TDO enzymes belong to immune checkpoints, which can catalyze the essential amino acid tryptophan (Trp) catabolism to N-formylkynurenine via the kynurenine (kyn) pathway [7–9]. It is known that IDO is monomeric and widely distributed in extrahepatic tissues [7–9], whereas TDO as a homotetramer almost expresses in the liver and regulates the levels of systemic Trp [10]. Apart from the liver, the brain was also detected to express TDO [11,12]. Previous research suggested that TDO could catabolize tryptophan in gliomas, accompanied by the protein level increase in human brain malignant tumor [13]. Interestingly, TDO was also found in other human cancers, including melanoma, hepatocarcinoma, lung cancer and bladder cancer, in which Trp can be catalyzed by TDO to degrade and accumulate as its bioactive metabolites [14]. A growing body of evidences has been implicated that TDO can counterbalance antitumor immune responses [14,15]. As a result, the number of effector T cells would decrease via cell cycle arrest and death, but the regulatory T cells increased [13–15]. All of these support tumor progression or/and metastasis, indicating that TDO can be involved in the phenomenon of immune tolerance. Thereby, TDO is a significant target for cancer treatments, especially in combination with a potent chemotherapeutic agent.

Platinum-based chemotherapeutic agents such as cisplatin (cis), carboplatin and oxaliplatin are the first-line anticancer drugs [16,17], which are widely used in clinical treatments with numerous cancers [18–21]. As a class of typical cytotoxic drugs, platinum(II)-based complexes induce cancer cell apoptosis through DNA damage [22,23]. However, their drawbacks like severe side effects, high toxicity, tumor recurrence and inherent/required drug resistances are obvious [17,22,24]. In order to overcome these shortcomings, Pt(IV) prodrugs have been applied, which can be effectively reduced to release active platinum(II) species by biomolecular agents such as ascorbic acid and glutathione [25–29]. To take the advantage of chemotherapy and

* Corresponding author at: Pharmaceutical Research Center and School of Chemistry and Chemical Engineering, Southeast University, Nanjing 211189, China.
E-mail address: sgou@seu.edu.cn (S. Gou).
[1] The first two authors contributed equally to the work.

https://doi.org/10.1016/j.jinorgbio.2019.02.004
Received 9 September 2018; Received in revised form 7 February 2019; Accepted 8 February 2019
Available online 12 February 2019
0162-0134/

immunotherapy, Lippard et al. reported a novel promising Pt(IV) prodrug conjugated with an IDO inhibitor that could effectively block IDO protein expression and result in T-cell activation and proliferation [30]. However, this strategy is still in a nascent area, especially Pt(IV) complexes containing TDO immune checkpoint inhibitors have not been reported.

Herein we reported a few Pt(IV) complexes derived from cisplatin containing a TDO inhibitor unit to enhance anticancer immune response. A key aspect of this strategy is expected to release cisplatin to induce cancer cell death by DNA damage, simultaneously generate the TDO inhibitor to block TDO protein expression to promote T cell proliferation and kill cancer cells, lead to improve the therapeutic efficacy of chemotherapeutic drugs.

2. Results and discussion

2.1. Synthesis and characterization

The TDO inhibitor (**1**) was synthesized according to a literature method [5]. Target Pt(IV) complexes **2** and **3** were obtained by treatment of **1** with Pt(IV) precursors in the presence of O-(benzotriazol-1-yl)-*N*,*N*,*N*′,*N*′-tetramethyluronium tetrafluoroborate (TBTU)/Et_3N (Scheme 1). All the resulting complexes were characterized by microanalysis, ^1H and ^{13}C NMR, and high resolution ESI-MS (Figs. S1–S8). All the spectral data were compatible with the target complexes **1–3**.

2.2. In vitro cytotoxicity

In vitro anticancer activity of complexes **2–3** was evaluated via 3-(4,5-dimethylthiazol-2-yl)-2,5-diphenyltetrazolium bromide (MTT) assays against a panel of cancer cells (HepG-2, A549, U87 in which TDO expressed, Fig. S11) together with normal liver cells LO2. Cisplatin and compound **1** were used as positive controls. The corresponding IC_{50} values were obtained following 72 h treatments with the tested samples. As listed in Table 1, compound **1** (IC_{50} values between 20.02 and 25.02 μM) showed relatively weaker antiproliferative activity than those Pt(IV) complexes against all the tested cancer cell lines, but exhibited the lowest cytotoxicity against normal LO2 cells. Notably, mono-modified Pt(IV) complexes **2** and **3** displayed strong antitumor activity comparable to cisplatin and cis/**1** mixture (1:1) against the tested cancer cells. Significantly among three complexes and cisplatin, complexes showed the weakest toxicity toward LO2 cells, especially complex **3** (1.06 μM) expressed the strongest cytotoxicity against HepG-2 cancer cells in which TDO was confirmed in high expression among the three cancer cells (Fig. S11).

Table 1
In vitro cytotoxicity of Pt(IV) complexes against human cancer cell lines.

Compound	IC_{50}(μM)[a]			
	HepG-2	A549	U87	LO2
1	21.97 ± 0.36	25.02 ± 1.21	20.02 ± 1.17	42.27 ± 2.36
2	5.23 ± 0.21	1.78 ± 0.12	1.59 ± 0.13	18.86 ± 0.53
3	1.06 ± 0.18	6.34 ± 0.44	2.94 ± 0.19	23.21 ± 0.27
cis	3.85 ± 0.11	2.74 ± 0.17	2.20 ± 0.17	10.89 ± 1.01
cis:**1** = 1:1	4.21 ± 0.19	1.88 ± 0.11	2.31 ± 0.11	17.96 ± 0.39

[a] The data represent the mean of at least three independent experiments.

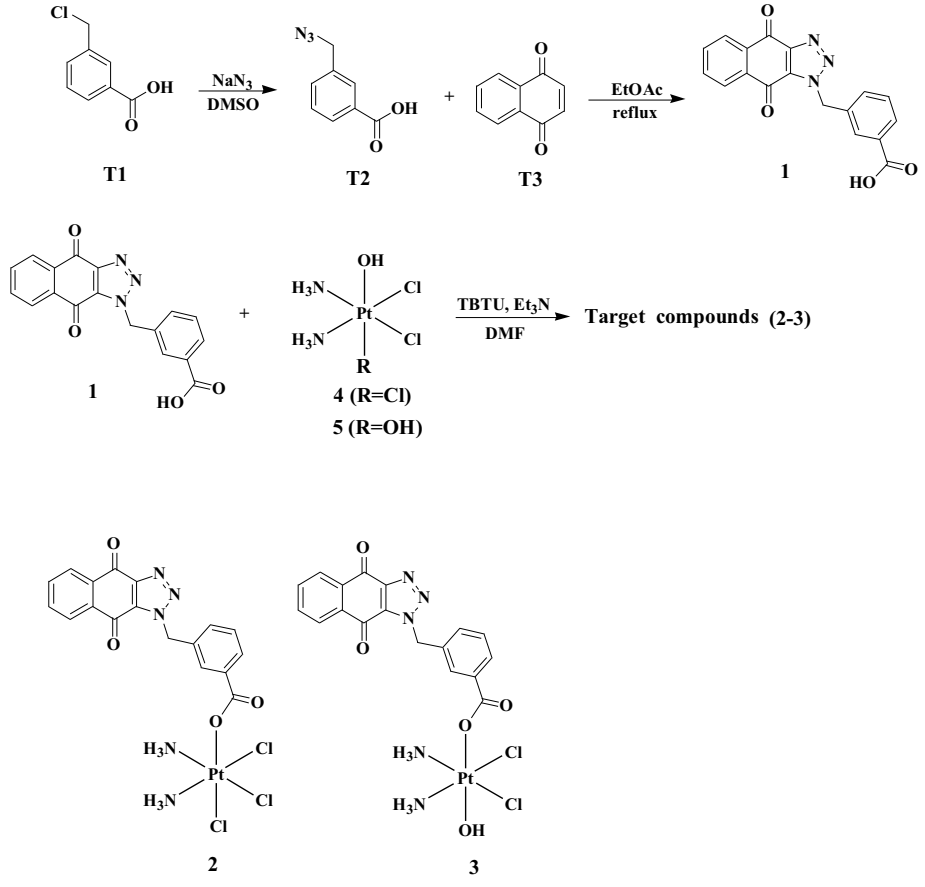

Scheme 1. Synthesis of Pt(IV) complexes **2** and **3**.

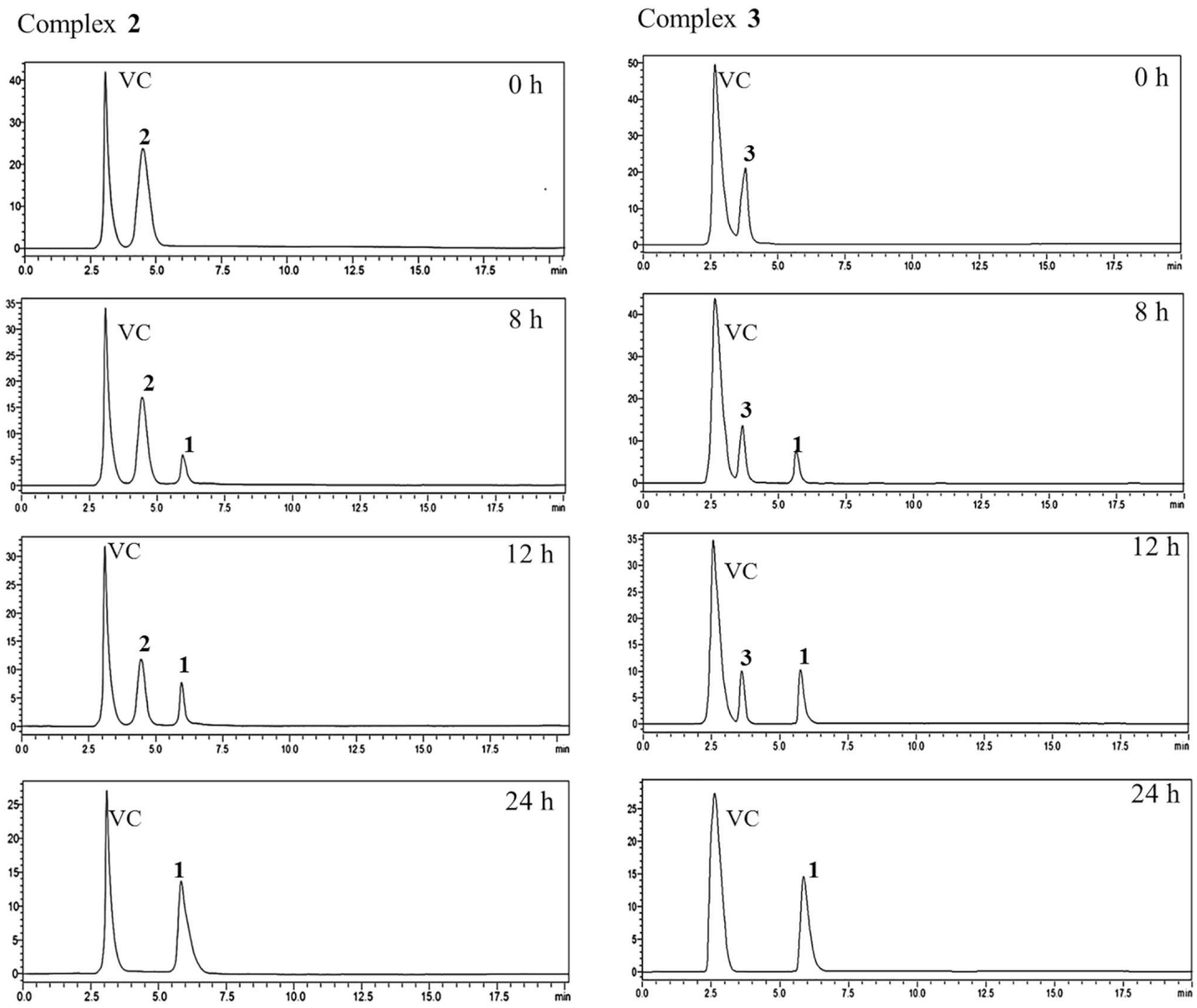

Fig. 1. The releasing ability of **2–3** under reduction with ascorbic acid (AA).

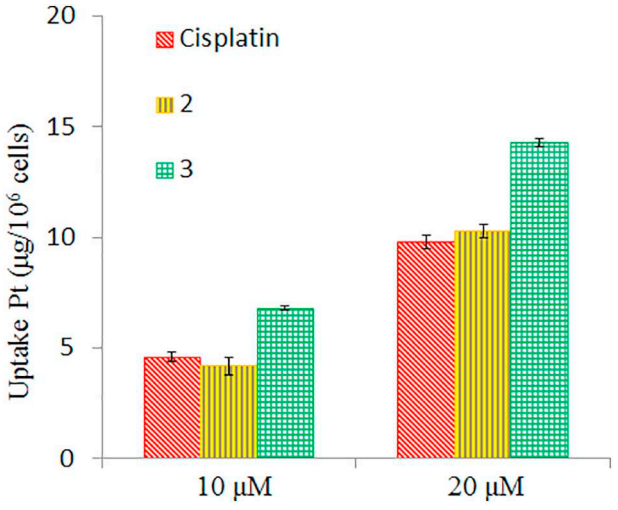

Fig. 2. Cell uptake of cisplatin, **2** and **3** in HepG-2 cells for 12 h. Results are expressed as the mean ± SD for three independent experiments.

*2.3. HPLC analyses on the stability of complexes **3** and the reduction of complexes **2–3***

Based on the above results the solution stability and the reduction of complexes were examined by High Performance Liquid Chromatography (HPLC) at different times. As shown in Fig. S12, HPLC data demonstrated that complex **3** in both phosphate buffered saline (PBS) (pH = 6.5 and 7.4) and serum solutions was stable in 48 h. To further confirm whether complexes **2** and **3** could be reduced to release its Pt(II) equivalent with the TDO inhibitor compound **1** in the presence of ascorbic acid (AA), complexes **2** and **3** were investigated by HPLC in a mixture solvent of acetonitrile/PBS (70%/30%, v/v) containing ascorbic acid. As shown in Fig. 1, complexes **2** and **3** were reduced in the presence of ascorbic acid to release the TDO inhibitor gradually as the time passed, accompanied by the peak of **2** and **3** falling down and the peak of compound **1** rising up, confirming that these compounds could be reduced to their Pt(II) equivalents. It was noted that cisplatin was not observed in the HPLC chromatograms due to its weak chromophore under the ultraviolet detecting conditions. These results suggested that the Pt(IV) complex **3** was stable in PBS and serum solutions, complexes **2** and **3** could be reduced to release the TDO inhibitor in the presence of

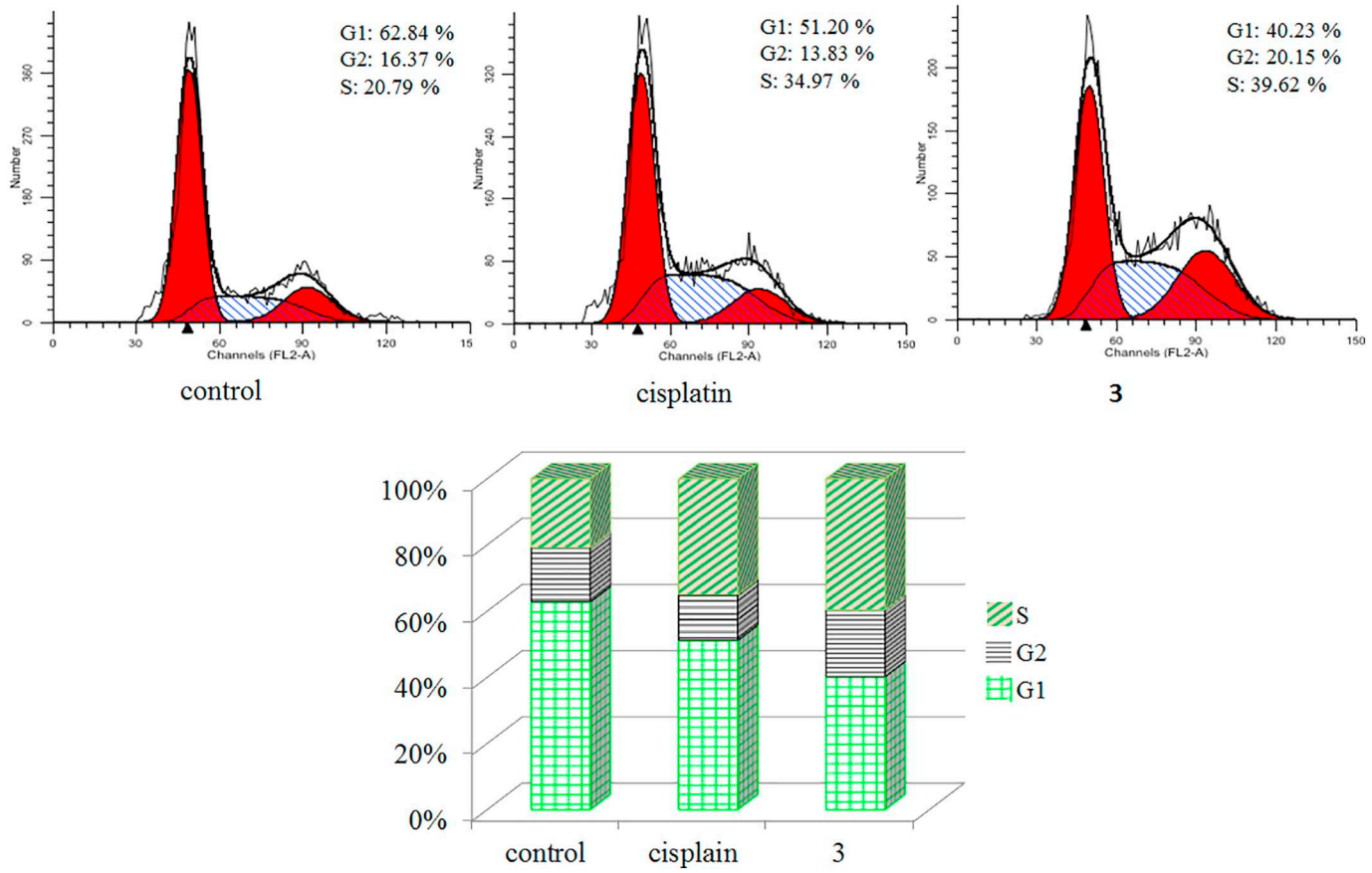

Fig. 3. Cell cycle distribution of HepG-2 cells after treated with cisplatin or **3** at 10 μM for 24 h. Data are expressed as the mean ± SEM for three independent experiments.

ascorbic acid.

2.4. Cellular uptake

The cellular accumulation of complexes **2** and **3** was measured in HepG-2 cells (high expression of TDO) by using the graphite furnace atomic absorption spectrometry (GFAAS) with cisplatin as a positive control. After treatment with the tested compounds (10 and 20 μM) for 12 h, the cellular platinum content in HepG-2 cells obviously increased in a concentration-dependent manner, suggesting facile internalization of these compounds within 12 h. As shown in Fig. 2 and Table S1, the platinum amount of complexes **2** and **3** in HepG-2 cells was significantly higher than that of cisplatin at two concentrations. Moreover, complex **3** with a hydroxy group could be more accumulated in HepG-2 cells than complex **2** with a chlorido ligand. Upon the cytotoxicity and cellular accumulation assay, it seems that the increased anticancer activity of complex **3** may be due to the improvement of cellular Pt uptake in comparison with cisplatin.

2.5. Effect on cell cycle arrest

To investigate the effect of complex **3** on cell cycle arrest, we used flow cytometry to analyze the cell cycle distribution of HepG-2 cells following a 24 h treatment with complex **3** at 10 μM. Untreated cells were used as a negative control, and cells treated with cisplatin were used as a positive control. As shown in Fig. 3, S phase cells markedly increased compared with the untreated group, and G1 period cells gradually decreased after treatment with complex **3**. The S phase cells increased from 20.79% (control) to 34.97% (cisplatin) and 39.62% (complex **3**), confirming complex **3** mainly arrested the cell cycle at S phase like cisplatin.

2.6. Apoptosis studies

The apoptosis of complex **3** in HepG-2 cells was studied by flow cytometry using Annexin V propidium iodide (PI) staining. The cancer cells were incubated with complex **3** at 5 μM for 24 h with cisplatin as a positive control. As showed in Fig. 4, both complex **3** and cisplatin significantly induced apoptosis. Specifically, compared with the apoptotic cells rate of the control (3.61%), the percentage of apoptosis cells was increased to (14.99%) after treatment with complex **3**, while cisplatin induced apoptosis at a ratio of 7.74%. The results indicated that complex **3** effectively caused apoptosis in HepG-2 cells superior to cisplatin.

2.7. Western blot analysis the effect of complex *3* on mitochondrial apoptosis pathway in HepG-2 cells

In order to investigate the mechanism of complex **3**, Bcl-2-associated X protein (Bax), B-cell lymphoma/leukemia 2 (Bcl-2), caspase-3 and poly ADP-ribose polymerase (PARP) proteins related to mitochondrial apoptotic pathways were detected in HepG-2 cells via western blot assay. As showed in Fig. 5, after treated with measured samples for 24 h, the protein expression of Bax was significantly increased and the level of Bcl-2 was reduced compared with the control. Interestingly, complex **3** induced the most meaningful regulation in the expression of Bax and Bcl-2, in which Bcl-2 was remarkably decreased, while Bax was greatly increased. The consequences resulted in the activation of caspase-3 and the cleavage of downstream apoptosome complex cleaved PARP which led to the final phase of cell death by a mitochondrial-mediated and caspase cascade pathway.

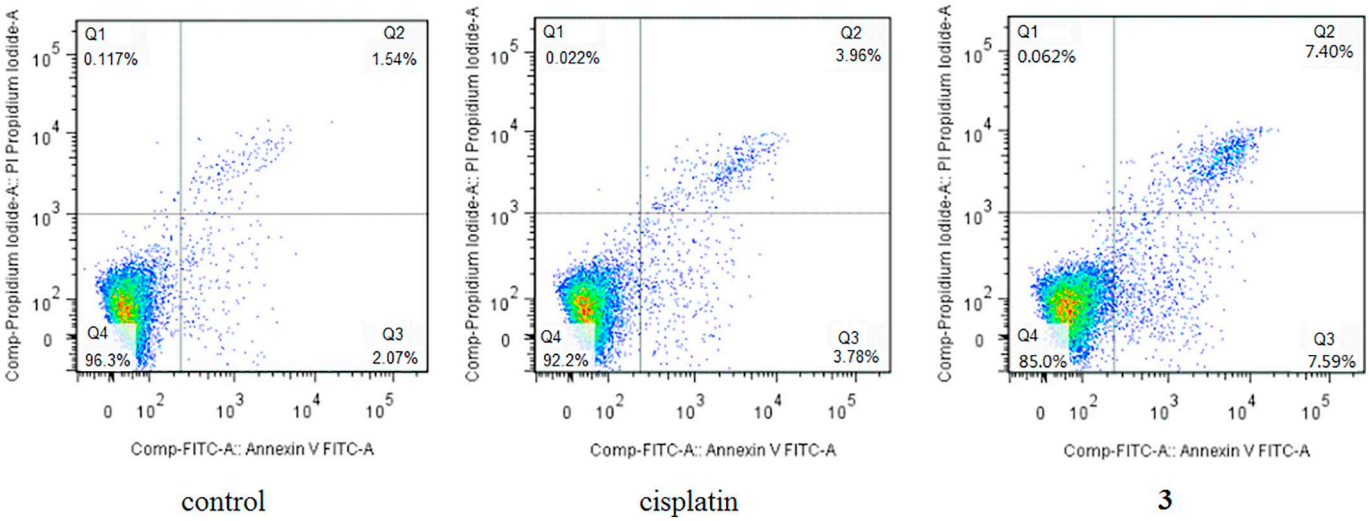

Fig. 4. Flow cytometric histograms of apoptotic HepG-2 cells after treated with cisplatin (5 μM) and **3** (5 μM) for 24 h. Lower left (Q4), living cells; lower right (Q3), early apoptotic cells; upper right (Q2), late apoptotic cells; upper left (Q1), necrotic cells. Inserted numbers in the profiles indicate the percentage of the cells present in this area. Data are expressed as the mean ± SEM for three independent experiments.

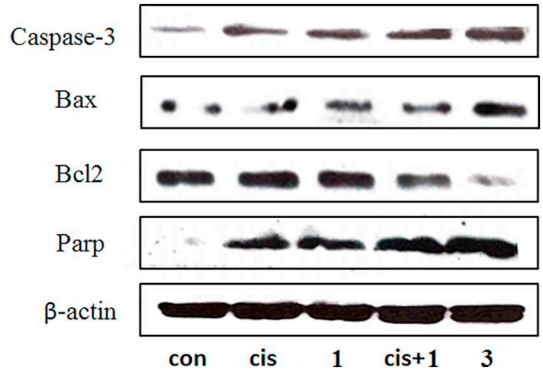

Fig. 5. Western blot analysis of the expression of related proteins with complex **3** at 10 μM for 24 h.

2.8. TDO and kynurenine inhibition assay

The mechanistic studies on the TDO pathway were performed after treated with complex **3**. As shown in Fig. 6A and Table S2, complex **3** displayed significant inhibitory potency of TDO enzyme with an IC_{50} value (0.85 μM) smaller than that of complex **2**. In view of the above data, complex **3** was selected for further research. The level of TDO expression after treatment with complex **3** was examined in HepG-2 cells. By using western blot and quantitative real time polymerase chain reaction (qRT-PCR) techniques, we found that complex **3** could effectively down-regulate TDO protein expression (Figs. 6B, 7 and S13). The results indicated that complex **3** could effectively block TDO, even stronger than compound **1**, in the cancer cells, while cisplatin had no ability to blockade TDO transcription or to induce TDO mRNA instability. The ability of complex **3** to suppress tryptophan to kynurenine production in HepG-2 cells was also detected by HPLC. The expression

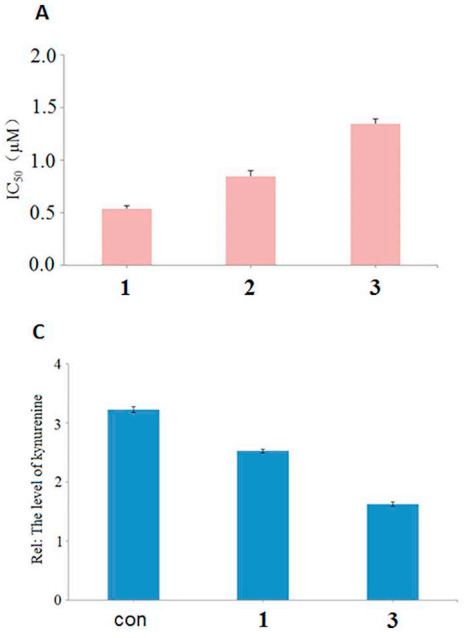

Fig. 6. (A) TDO inhibitory potency (IC_{50} data) of compounds **1**, **2** and **3**. (B) Western blot analysis of TDO expression in HepG-2 cancer cells after treated with measured compounds at 10 μM for 24 h. (C) Kynurenine inhibition of **1** and **3** (10 μM) assessed by HPLC. Results are expressed as the mean ± SD for three independent experiments. $P < 0.05$.

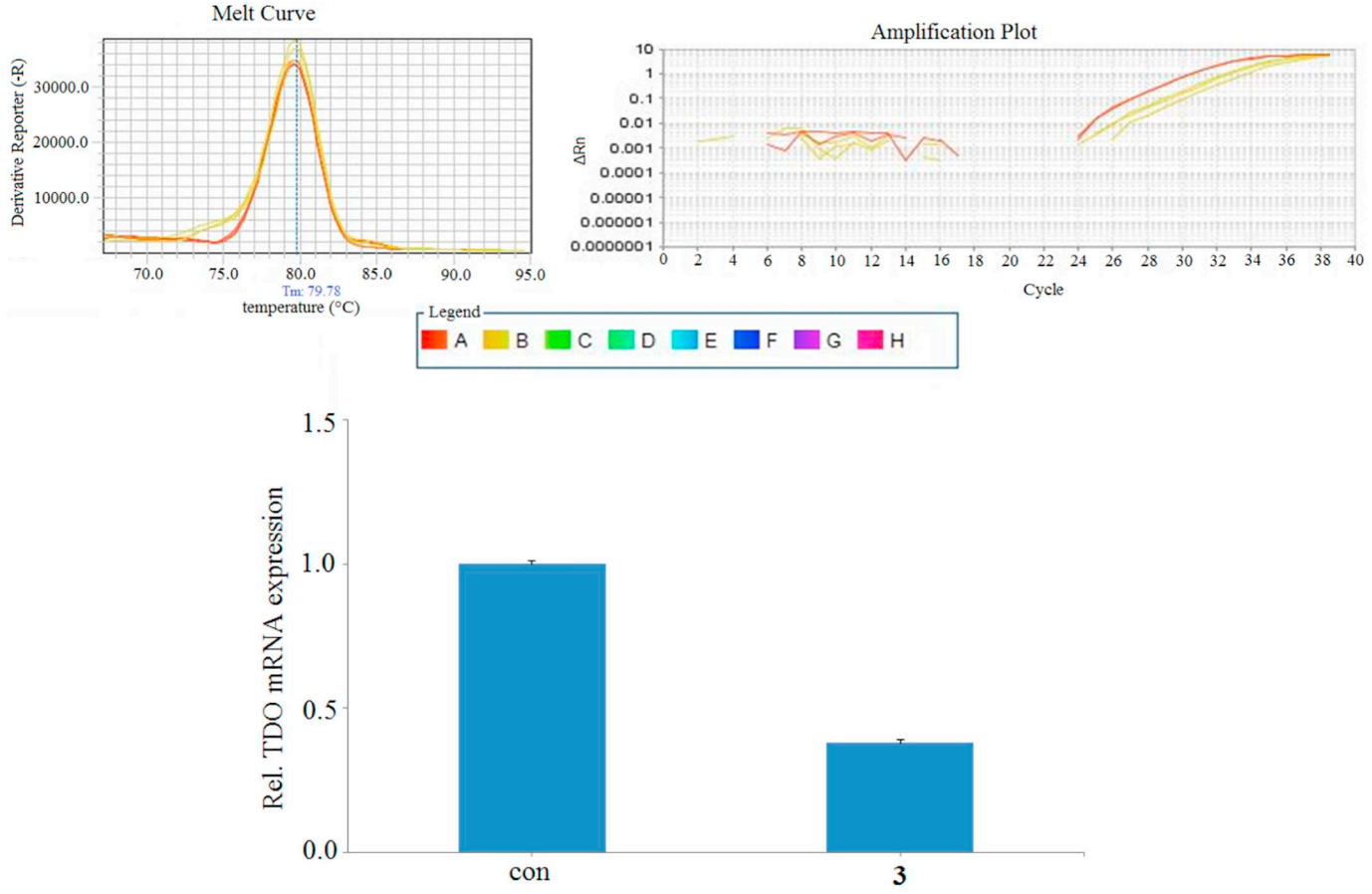

Fig. 7. qRT-PCR of mRNA expression level of TDO after exposure to **3** (10 μM) in HepG-2 cells for 24 h. $P < 0.05$.

levels of Trp and kynurenine were showed in Figs. 6C and S14. The TDO inhibitor, compound **1**, could effectively block the kynurenine production as expected, in which group the level of Trp was higher than that of kynurenine. Intriguingly, **3** showed stronger inhibition ability than **1**, because the level of kynurenine in the complex **3** group was even lower than that in the compound **1** group. Taken together, these results demonstrated that complex **3** could interrupt the kynurenine pathway by inhibiting TDO enzyme activity.

2.9. AHR inhibition assay

Aryl hydrocarbon receptor (AHR) is a cytosolic transcription factor which can be activated by the xenobiotic ligands kynurenine and then accumulated to the nucleus. The accumulation of AHR in nucleus leads to promote tumor growth and suppress antitumor immune responses [13]. As illustrated in Fig. 6, complex **3** could inhibit TDO expression and block the kynurenine production, which may lead to the inactivation of AHR. To further study the mechanism of complex **3** via the TDO pathway, we examined the expression of AHR by quantitative (q) RT-PCR. After treated with complex **3** in HepG-2 cells for 24 h, the RNA was harvested to be detected with real time polymerase chain reaction (PCR). As shown in Fig. 8, complex **3** could effectively decrease mRNA expression levels of AHR in comparison with the control. These results indicated that complex **3** could interrupt the TDO–Kyn–AHR signal pathway and lead to inactivate the downstream of AHR.

2.10. T-cell proliferation

As kynurenine (Kyn), the bioactive metabolite of Trp, can suppress T-cell proliferation [31], we studied the immunostimulatory potential of complex **3** in vitro via the mixed leukocyte reaction (MLR) that was used for assessing the immune response. The immune T-cell proliferation was examined by flow cytometry after co-cultured with adherent HepG-2 cells and treated with complex **3**. In the experiment, peripheral blood mononuclear cells (PBMCs) from healthy donors were pretreated and co-cultured with HepG-2 cells. The HepG-2/MLRs were treated with complex **3** for 6 days, the medium was centrifugated to harvest PBMCs, T-cell proliferation was detected by flow cytometry after stained with APC-anti CD4/PE-anti CD8 and FITC-conjugated anti-CD3 antibody. As showed in Figs. 9 and S15, the HepG-2/MLR incubated with cisplatin showed insignificantly T-cell proliferation. Compound **1** and the mixture of **1** and cisplatin displayed potent to boost T-cell proliferation. Interestingly, complex **3** displayed the most potential to enhance T-cell proliferation compared to the other treatments. Collectively, these results confirmed that complex **3** not only inhibits tumor cell growth directly, but also stimulates T cell proliferation as an immuno-chemotherapeutic agent to attack the cancer cells.

3. Conclusions

In summary, we present the first example of Pt(IV) complexes containing a small-molecule TDO inhibitor as an immune-chemotherapeutic agent. Cytotoxicity assay showed that these Pt(IV) complexes displayed significantly antitumor activities against the tested cancer cells with low toxicity toward the normal human liver cell LO2. Especially, complex **3** exhibited excellent cytotoxicity against the TDO highly expressed HepG-2 cells. As a Pt(IV) prodrug, complex **3** can be activated to release active platinum(II) species and the TDO Inhibitor by intracellular reduction as expected. The anticancer effect of complex **3** was investigated by the synergy of cisplatin and the TDO inhibitor. The result evidenced that complex **3** could induce cell death via a mitochondrial-dependent apoptosis pathway and arrest the cell cycle at S

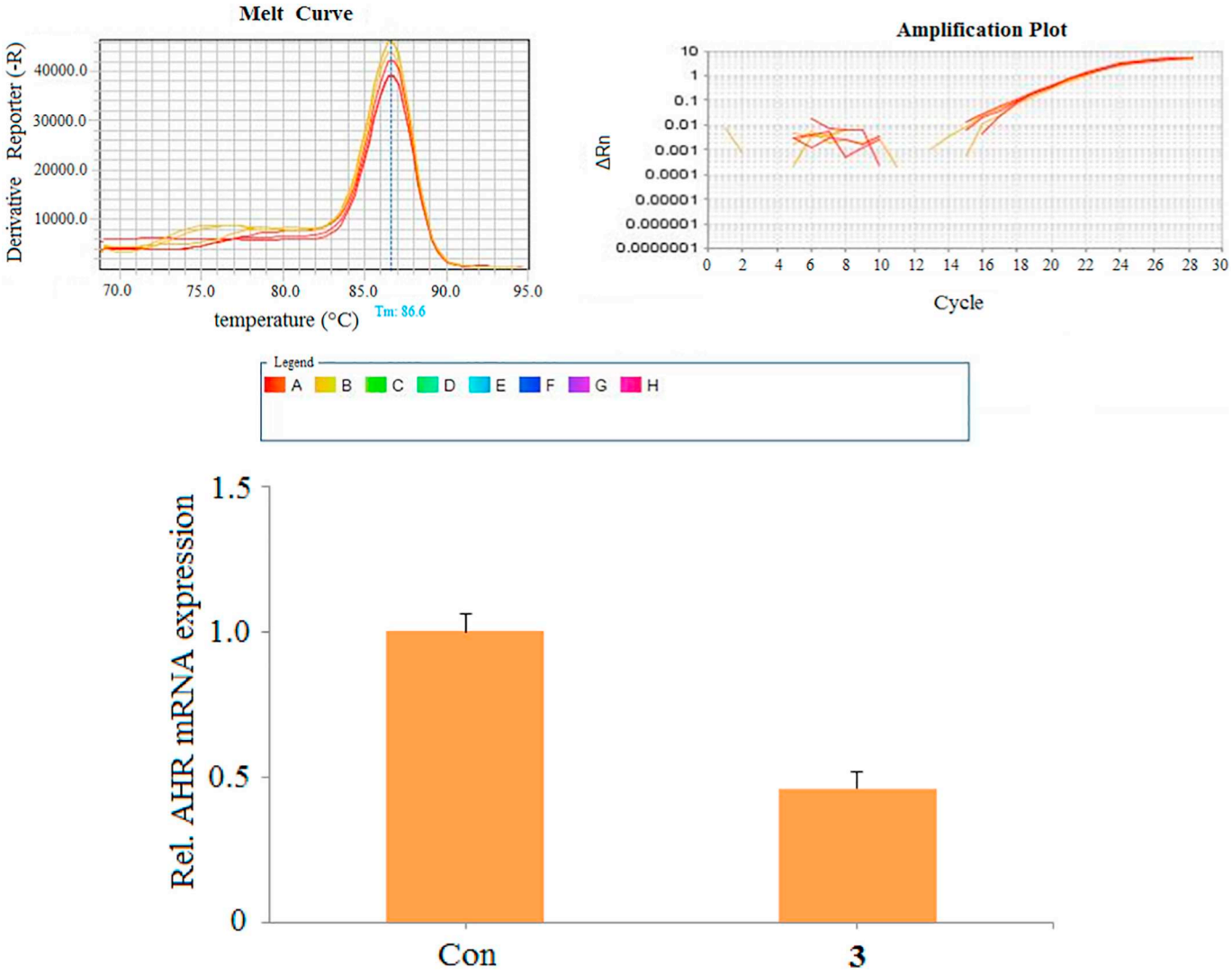

Fig. 8. qRT-PCR of mRNA expression level of AHR after exposure to **3** (10 μM) in HepG-2 cells for 24 h. Results are expressed as the mean ± SD for three independent experiments. $P < 0.05$.

phase. Furthermore, the immunosuppressive enzyme TDO expression was effectively inhibited by complex **3** which led to the blockade of Kyn production and inactivation of AHR. This action improved tumor immune microenvironment and significantly enhanced T-cell proliferation. In conclusion, combination of chemotherapeutic drugs with immune checkpoint inhibitors may provide a significant approach for immune-chemotherapy in cancer treatment. However, the synergy of TDO inhibitors and platinum-based drugs and related intensive mechanism need to be studied in future.

4. Materials and methods

4.1. Materials and instrument

Platinum(IV) precursors as well as the TDO Inhibitor (compound **1**) were prepared according to literature reports [5,32]. All the chemical reagents and solvents used were of analytical grade and used without further purification, unless noted specifically. The purity of all compounds used in the biophysical and biological studies was ≥95%. All cancer cell lines were obtained from Jiangsu KeyGEN BioTECH company (China). ^{1}H and ^{13}C NMR were recorded on a BRUKER AV-400 spectrometer with tetramethylsilane (TMS) as an internal standard in DMSO. Mass spectra were measured with an Agilent 6224 TOF LC/MS instrument. Platinum contents were detected by Atomic Absorption Spectrometer (AAS, Hitachi, Japan). Peripheral blood mononuclear cells (PBMCs) from unrelated healthy donators. Anti-CD4/8 antibody (Abcam), FITC-conjugated anti-CD3 antibody and anti-TDO2 were purchased for flow cytometry study. The Acitn, Bax, Bcl-2, caspase-3, PAPR antibodies were purchased from Imgenex, USA.

4.2. Synthesis and characterization

Synthesis of 1: A solution of sodium azide (0.97 g, 14.9 mmol) and 3-(chloromethyl)-benzoic acid (**T1**) (1.70 g, 10.0 mmol) in 10 mL of DMSO was stirred for 5 h at room temperature. After completion of reaction, the reaction mixture was quenched by adding water and extracted with ethyl ether to give the desired product **T2**. The azido compound **T2** (1.50 g, 8.5 mmol) was stirred with 1, 4-naphthoquinone (**T3**) (2.01 g, 12.7 mmol) in the presence of ethyl acetate at 77 °C. After cooling, the mixture was filtered and washed with ethanol to give the desired product **1** as a yellow-brown solid (1.40 g, 40%). ^{1}H NMR (400 MHz, DMSO) δ 8.22–8.15 (m, 2H), 8.04 (s, 1H), 7.97–7.90 (m, 3H), 7.65 (d, J = 8.2 Hz, 1H), 7.52 (m, J = 7.7 Hz, 1H), 6.11 (s, 2H). HRMS (FAB) m/z calcd for $C_{18}H_{11}N_3O_4$ (M): 333.0750, found $[M-H]^-$ = 332.0938.

Synthesis of 2: A solution of compound **1** (120 mg, 0.36 mmol),

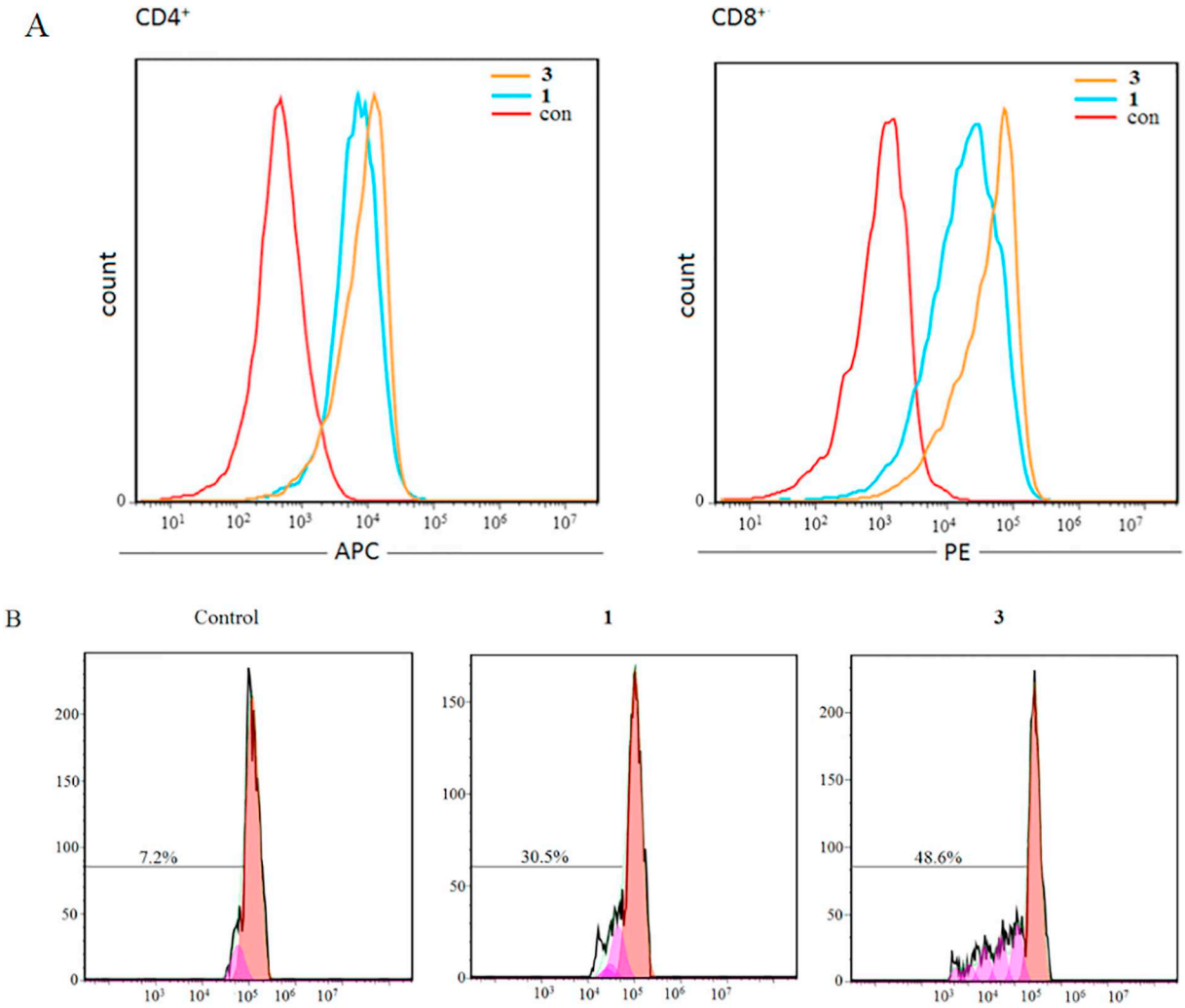

Fig. 9. Mixed leukocyte reactions to estimate T-cell proliferation after measured compounds (10 μM) incubated with PBMCs and HepG-2 cells by measuring cell marker CD4/8$^+$ (A) and CFSE-labeled CD3$^+$ T (B) cells using flow cytometry.

TBTU (173 mg, 0.54 mmol), and Et_3N (55 mg, 0.54 mmol) in dry DMF (6 mL) was stirred at room temperature under N_2 atmosphere for 10 min, c,c,t-[$Pt(NH_3)_2Cl_3(OH)$] (150 mg, 0.42 mmol) was added in portions. The mixture was stirred at room temperature overnight. After completion of reaction, the whole mixture was concentrated under reduced pressure. The residue was purified on silica gel column eluted DCM/MeOH (30:1) to give the desired product 2 as a yellow solid (91.1 mg, 33.7%). ^{1}H NMR (400 MHz, DMSO) δ 8.23 (d, J = 7.2 Hz, 1H), 8.19 (d, J = 7.0 Hz, 1H), 8.00–7.94 (m, 3H), 7.86 (d, J = 7.7 Hz, 1H), 7.56 (d, J = 7.4 Hz, 1H), 7.47 (m, J = 7.7 Hz, 1H), 6.38 (s, 6H), 6.11 (s, 2H). ^{13}C NMR (100 MHz, DMSO) δ 177.32, 175.59, 172.98, 145.46, 135.63, 135.00, 134.95, 134.37, 133.70, 133.37, 131.67, 130.11, 129.43, 128.95, 127.46, 127.36, 53.17. HRMS (FAB) m/z calcd for $C_{18}H_{16}Cl_3N_5O_4Pt$ (M): 667.7877, found [M-H]$^-$ = 666.0283. Elemental analysis calcd (%) for $C_{18}H_{16}Cl_3N_5O_4Pt$: C, 32.37; H, 2.41; N, 10.49; found: C, 32.25; H, 2.60; N, 10.35.

Synthesis of 3: A solution of compound 1 (120 mg, 0.36 mmol), TBTU (173 mg, 0.54 mmol), and Et_3N (55 mg, 0.54 mmol) in dry DMF (6 mL) was stirred at room temperature under N_2 atmosphere for 10 min, c,c,t-[$Pt(NH_3)_2Cl_2(OH)_2$] (132 mg, 0.40 mmol) was added in portions. The mixture was stirred at room temperature overnight. After completion of reaction, the whole mixture concentrated under reduced pressure. The residue was purified on silica gel column eluted DCM/MeOH (20:1) to give the desired product 3 as a yellow solid (45 mg, 20%). ^{1}H NMR (400 MHz, DMSO) δ 8.18 (dd, J = 7.4, 1.2 Hz, 1H, H-4), 8.17 (dd, J = 7.4, 1.4 Hz, 1H, H-1), 7.97–7.92 (m, 3H, H-2, H-3, H-5), 7.85 (d, J = 7.7 Hz, 1H, H-6), 7.48 (d, J = 7.7 Hz, 1H, H-8), 7.40 (m, J = 13.4, 5.7 Hz, 1H, H-7), 6.45–6.09 (m, 6H, 2-NH_3), 6.07 (s, 2H, H-9). ^{13}C NMR (100 MHz, DMSO) δ 176.92, 175.15, 173.00, 145.02, 135.44, 135.19 (CH, C-3), 134.57 (CH, C-4), 134.34, 133.92, 133.26, 132.94, 130.81 (CH, C-6), 129.59 (CH, C-8), 128.96 (CH, C-5), 128.35 (CH, C-7), 127.00 (CH, C-2), 126.94 (CH, C-1), 52.79 (CH_2, C-9). HRMS (FAB) m/z calcd for $C_{18}H_{17}Cl_2N_5O_5Pt$ (M): 649.3241, found [M-H]$^-$ = 648.0281. Elemental analysis calcd (%) for $C_{18}H_{17}Cl_2N_5O_5Pt$: C, 33.29; H, 2.64; N, 10.79; found: C, 33.12; H, 2.75; N, 10.63.

4.3. Cell culture

The following in vitro human cancer cell lines were used: HepG-2 (human hepatoma cancer cell), A549 (human lung cancer cell line), U87 (human primary glioblastoma cell line), LO2 (normal human liver cell) were maintained in monolayer culture in Dulbecco's modified Eagle medium (DMEM) medium containing 10% fetal bovine serum (FBS), 100 mg/mL of penicillin and 100 mg/mL of streptomycin, kept in a humidified incubator with 5% CO_2 at 37 °C.

4.4. Cytotoxicity analysis

The MTT method was used to evaluate the antitumor activity of all tested complexes. Briefly, about 5 × 10^4 cells/mL cells were seeded in

each well of 96-well plates in DMEM medium with 10% FBS and incubated for 12 h at 37 °C in 5% CO_2. All tested compounds were prepared at five different concentrations, and then added to the test well, the cells were incubated at 37 °C in a 5% CO_2 atmosphere for another 72 h. After 72 h, the cells were treated with a 0.5 mg/mL solution of MTT and the plate was incubated for an additional 4 h. The medium was thrown away and 100 μL of DMSO was added. The O.D. value was read at 570/630 nm enzyme labeling instrument. The IC_{50} values were calculated by the Bliss method and repeated in three times.

4.5. The stability of **3** and releasing ability of **2** and **3**

The stability and released ability of Pt(IV) complexes in a solvent were detected by HPLC. As for the released analysis, the standard compounds were prepared in a solvent containing 70% acetonitrile and 30% PBS (0.5 M) with adding ascorbic acid (3 mM), compound **1** (1 mM), and Pt(IV) complexes (1 mM), respectively. The incubation was performed by adding test compounds to a solvent containing acetonitrile and PBS, which was detected by HPLC at different instants of time at 25 °C, respectively. As for the stability analysis, **3** was dissolved in DMF (0.5 mL) and diluted to a final concentration of 1 or 0.5 mM in a solvent of PBS or serum, which was detected by HPLC at different instants of time at 25 °C. The serum samples were dealt with according to the method of literature reports [33]. The serum samples were extracted with chloroform by vortexing at maximal speed for 1 min on a Vortex-Genie. The two layers were separated by centrifugation at 10,000 rpm for 5 min. Finally, the chloroform layer was injected into the chromatographic system. Reversed phase HPLC was implemented on a 250 × 4.5 mm ODS column and the HPLC profiles were recorded on UV detection at 245 nm. Mobile phase consisted of acetonitrile/water (70:30, v/v), and flow rate was 1.0 mL/min. The samples were taken for HPLC analysis after filtration by 0.45 μm filter.

4.6. Cellular uptake analysis

HepG-2 cells were seeded in 6-well plates and incubated until the cells reached about 80% confluence. Then, cells were treated with the test compounds (10 μM, 20 μM) and subsequently incubated at 37 °C for 12 h. After completion of 12 h incubation, the medium was removed, cells were collected and washed three times with ice-cold PBS. The cell suspension was centrifuged in an Eppendorf tube for 5 min and resuspended in 1 mL PBS. A volume of 100 μL was taken out to determine the cell density. The rest of cells were digested at 65 °C in 200 μL 65% HNO_3 for 12 h. The platinum content in cells was analyzed by graphite furnace atomic absorption spectrometry (GFAAS).

4.7. Cell cycle analysis

HepG-2 cells were seeded in 6-well plates and treated with indicated concentrations of complex **3** and cisplatin. After incubated in 5% CO_2 at 37 °C for 24 h, cells were washed twice with ice-cold PBS, fixed and permeabilized with ice-cold 70% ethanol at −20 °C overnight. The cells were treated with 100 mg/mL RNase A at 37 °C for 30 min after washed with ice-cold PBS, and finally stained with 1 mg/mL propidium iodide (PI) in the dark at 4 °C for 30 min. Analysis was performed with the system software (Cell Quest; BD Biosciences).

4.8. Apoptosis analysis

Apoptosis was evaluated by flow cytometry analysis of Annexin V staining. HepG-2 Cells were seeded at the density of 2×10^6/well in 10% FBS-DMEM into 6-well plates to the final volume of 2 mL, and treated with complex **3** and cisplatin for 24 h. The cells were collected and washed twice with cold phosphate buffered saline (PBS) and then resuspend cells in 1 × Binding Buffer (0.1 M Hepes/NaOH (pH 7.4), 1.4 M NaCl, 25 mM $CaCl_2$) at a concentration of 1×10^6 cells/mL. Transfer 100 μL of the solution to a 5 mL culture tube, and add 5 mL of FITC Annexin V (BD, Pharmingen) and 5 mL propidium iodide (PI) to each tube. Gently vortex the cells and incubate for 30 min at room temperature (25 °C) in the dark. Add PBS to each tube. Analysis was performed with the system software (Cell Quest; BD Biosciences).

4.9. Western blot analysis

The western blotting procedure was performed as described previously [34]. HepG-2 cells were treated with the test complex **3** and positive drugs at indicated concentrations for 24 h. After for 24 h, cells were collected, centrifuged, and washed twice with ice-cold PBS. The pellets were then resuspended in lysis buffer. After the cells were lysed in ice lysis buffer for 30 min, lysates were centrifuged at 4 °C for 10 min. The protein concentration in the supernatant was detected by the BCA protein assay reagents. Equal amounts of protein per line was separated on 12% SDS polyacrylamide gel electrophoresis and transferred to PVDF Hybond-P membrane (GE Healthcare). Membranes were incubated with 5% skim milk in Tris-buffered saline with Tween 20 (TBST) buffer for 1 h and then the membranes being gently rotated overnight at 4 °C. Membranes were then incubated with primary antibodies at 4 °C for overnight. Next, membranes incubated with peroxidase labeled secondary antibodies for 2 h and washed with TBST four times for 20 min. The protein blots were detected by chemiluminescence reagent (Thermo Fischer Scientifics Ltd.). The X-ray films were developed with developer and fixed with fixer solution.

4.10. TDO enzyme assays

The TDO enzymatic inhibition assays were performed as previous described [35] and manufacturer's instructions. Due to N-formylkynurenine has an absorbance peak at 321 nm; thus, the TDO activity was evaluated via the detection of the 321 nm peak in the reaction mixtures by spectral analysis. Briefly, after thawing, the TDO reaction solution was added into each well of 96-well plates, and 10 μL of test inhibitor solution was added to each well as the “Test Inhibitor”, with 10 μL of the same solution without inhibitor as the “Positive Control” and “Blank”. Then, add 10 μL of TDO, His-tag solution (dilute TDO, His-tag in 1 × TDO Assay Buffer as 50 ng/μL solution) to the wells labeled “Positive Control,” and “Test Inhibitor”, and add 10 μL of 1 × TDO Assay Buffer to the “Blank” well. The reaction mixtures was incubated at room temperature for 90 min to measure absorption at $\lambda = 321$ nm by spectral analysis.

4.11. Determination of tryptophan and kynurenine level in HepG-2 by HPLC

The level of tryptophan and kynurenine was performed as described previously [30]. HepG-2 cells were plated at 2×10^5 cells in a 6-well plate with 2 mL medium for kynurenine and tryptophan concentrations Determination. After treated with the test compounds for 48 h, the medium was harvested, centrifuged, and frozen for further analysis. After the cells thawing, the 20% trichloroacetic acid was added for protein precipitation, then the sample was centrifuged, and 100 μL of the supernatant was analyzed by HPLC. Reversed phase HPLC was implemented on a 250 × 4.5 mm ODS column and the HPLC profiles were recorded on UV detection at 360 nm. Mobile phase consisted of acetonitrile/water, and flow rate was 1.0 mL/min. The samples were taken for HPLC analysis after filtration by 0.45 μm filter.

4.12. Quantitative (q)RT-PCR

The quantitative real time polymerase chain reaction (qRT-PCR) of mRNA expression level of TDO and AHR was measured according to literature reports [30]. After treated with complex **3**, HepG-2 cells were collected to obtain the RNA for further analysis. Total RNA was isolated

with the Qiagen RNAeasy kit and cDNA was synthesized with the Applied Biosystems reverse-transcription-kit (Foster City, CA, USA). (q) RT-PCR was performed in a Light cycler 480 II thermo cycler with SYBR Green PCR Mastermix (Roche). All primers were separated by at least one intron on the genomic DNA to exclude its amplification. PCR reactions were checked by including no-RT controls, by omission of templates, and by melting curves. Standard curves were generated for each gene. Relative quantification of gene expression was determined by comparison of threshold values. All samples were analyzed in duplicate at two different dilutions. All results were normalized to glyceraldehyde-3-phosphate dehydrogenase (GAPDH). Primer sequences were (5′-3′ forward, reverse):

TGTTGCCATCAATGACCCCTT;CTCCACGACGTACTCAGCG (GAPDH)
GGCCGTGTCGATGTATCAGT; GCCTGGCAGTACTGGATTGT (AHR)
CGGTGGTTCCTCAGGCTATC; CTTCGGTATCCAGTGTCGGG (TDO)

4.13. Mixed leukocyte reaction to estimate T-cell proliferation

A mixed leukocyte reactions (MLRs) was performed as described previously [36,37]. HepG-2 cells were seeded in 6-well plates with a density of 1×10^5 cells/well. After cultivation for 24 h, the cells were replaced with fresh complete DMEM and treated with various test compounds with an untreated group as control. The HepG-2 cells were exposed to different compounds for 2 days at 37 °C. PBMCs (2×10^5 cells/well) stained with CellTrace™ Far Red Cell Proliferation Kit (CFSE) was subsequently inserted after phytohemagglutinin (PHA-M) stimulation. After co-culture for 6 days at 37 °C, the PBMCs were harvested, centrifugation and collected for further analysis. The cell pellets were resuspended in PBS and staining with APC-anti CD4/PE-anti CD8 antibody and FITC-conjugated anti-CD3 antibody. After staining with antibody, the T-cell proliferation was measured by flow cytometry.

Abbreviations

AA	ascorbic acid
AHR	aryl hydrocarbon receptor
Bax	Bcl-2-associated X protein
Bcl-2	B-cell lymphoma/leukemia 2
CFSE	carboxyfluorescein succinimidyl ester
DCM	dichloromethane
DMEM	Dulbecco's modified Eagle medium
DMF	*N*,*N*-dimethylformamide
DMSO	dimethylsulfoxide
Et_3N	triethylamine
FBS	fetal bovine serum
GAPDH	glyceraldehyde-3-phosphate dehydrogenase
GFAAS	graphite furnace atomic absorption spectrometry
HPLC	High Performance Liquid Chromatography
kyn	kynurenine
MLRs	mixed leukocyte reactions
MTT	3-(4,5-dimethylthiazol-2-yl)-2,5-diphenyltetrazolium bromide
PARP	poly ADP-ribose polymerase
PBS	phosphate buffered saline
PBMCs	peripheral blood mononuclear cells
PCR	polymerase chain reaction
PHA-M	phytohemagglutinin
PI	propidium iodide
qRT-PCR	quantitative real time polymerase chain reaction
TBST	Tris-buffered saline with Tween 20
TBTU	O-(benzotriazol-1-yl)-*N*,*N*,*N*′,*N*′-tetramethyluronium tetrafluoroborate
Trp	tryptophan
TMS	tetramethylsilane

Acknowledgments

We are grateful to the National Natural Science Foundation of China (Grant Nos. 21571033 and 81503099) for financial aids to this work. The research was also supported by Jiangsu Province Natural Science Foundation (Grant no. BK20150643). The authors would also like to thank the Fundamental Research Funds for the Central Universities (Project 2242017K41024) for supplying basic facilities to our key laboratory.

Appendix A. Supplementary information

Diagrams of ESI-MS, ^1H, and ^{13}C spectra. HPLC analyses on the stability of Pt(IV) complexes under reduction with ascorbic acid. Western blot expression of TDO, kynurenine inhibition, mixed leukocyte reaction to estimate T-cell proliferation and platinum contents data. This material is available free of charge via the Internet.

References

[1] J.C. Frankel, Science 342 (2013) 1432–1433.
[2] M.S. Kim, J.S. Ma, H. Yun, Y. Cao, J.Y. Kim, V. Chi, D. Wang, A. Woods, L. Sherwood, D. Caballero, J. Gonzalez, P.G. Schultz, T.S. Young, C.H. Kim, J. Am. Chem. Soc. 137 (2015) 2832–2835.
[3] B.S.L. Topalian, J.M. Taube, R.A. Anders, D.M. Pardoll, Nat. Rev. Cancer 16 (2016) 275–287.
[4] L.P. Kane, J. Immunol. 184 (2010) 2743–2749.
[5] J.S. Wu, S.Y. Lin, F.Y. Liao, W.C. Hsiao, L.C. Lee, Y.H. Peng, C.L. Hsieh, M.H. Wu, J.S. Song, A. Yueh, C.H. Chen, S.H. Yeh, C.Y. Liu, S.Y. Lin, T.K. Yeh, J.T. Hsu, C. Shih, S.H. Ueng, M.S. Hung, S.Y. Wu, J. Med. Chem. 58 (2015) 7807–7819.
[6] P. Sharma, J.P. Allison, Science 348 (2015) 56–61.
[7] S.J. Thackray, C.G. Mowat, S.K. Chapman, Biochem. Soc. Trans. 36 (2008) 1120–1123.
[8] R. Schwarcz, J.P. Bruno, P.J. Muchowski, H.Q. Wu, Nat. Rev. Neurosci. 139 (2012) 465–477.
[9] A. Curti, S. Trabanelli, V. Salvestrini, M. Baccarani, R.M. Lemoli, Blood 113 (2009) 2394–2401.
[10] W.E. Knox, A.H. Mehler, J. Biol. Chem. 187 (1950) 419–430.
[11] M. Kanai, H. Funakoshi, H. Takahashi, T. Hayakawa, S. Mizuno, K. Matsumoto, T. Nakamura, Mol. Brain. 2 (2009) 1–16.
[12] A. Maeta, T. Fukuwatari, H. Funakoshi, T. Nakamura, K. Shibata, Int. J. Tryptophan Res. 6 (2013) 55–65.
[13] C.A. Opitz, U.M. Litzenburger, F. Sahm, M. Ott, I. Tritschler, S. Trump, T. Schumacher, L. Jestaedt, D. Schrenk, M. Weller, M. Jugold, G.J. Guillemin, C.L. Miller, C. Lutz, B. Radlwimmer, I. Lehmann, A. Deimling, W. Wick, M. Platten, Nature 478 (2011) 197–203.
[14] L. Pilotte, P. Larrieu, V. Stroobant, D. Colau, E. Dolusic, R. Frederick, E.D. Plaen, C. Uyttenhove, J. Wouters, B. Masereel, B.J. VandenEynde, Proc. Natl. Acad. Sci. U. S. A. 109 (2012) 2497–2502.
[15] S.K. Schmidt, A. Müller, K. Heseler, C. Woite, K. Spekker, C.R. MacKenzie, W. Däubener, Eur. J. Immunol. 39 (2009) 2755–2764.
[16] X.Y. Wang, X.H. Wang, Z.J. Guo, Acc. Chem. Res. 48 (2015) 2622–2631.
[17] M. Galanski, M.A. Jakupec, B.K. Keppler, Curr. Med. Chem. 12 (2005) 2075–2094.
[18] L. Kelland, Nat. Rev. Cancer 7 (2007) 573–584.
[19] M.A. Fuertes, C. Alonso, J.M. Perez, Chem. Rev. 103 (2003) 645–662.
[20] D. Shen, I. Pastan, M.M. Gottesman, Cancer Res. 58 (1998) 268–275.
[21] F.F. Liu, S.H. Gou, F.H. Chen, L. Fang, J. Zhao, J. Med. Chem. 58 (2015) 6368–6377.
[22] D. Wang, S.J. Lippard, Nat. Rev. Drug Discov. 4 (2005) 307–320.
[23] E.R. Jamieson, S.J. Lippard, Chem. Rev. 99 (1999) 2467–2498.
[24] Z.H. Siddik, Oncogene 22 (2003) 7265–7279.
[25] Y. Yuan, R.T.K. Kwok, B.Z. Tang, B. Liu, J. Am. Chem. Soc. 136 (2014) 2546–2554.
[26] X.P. Han, J. Sun, Y.J. Wang, Z.G. He, Med. Res. Rev. 35 (2015) 1268–1299.
[27] L.L. Ma, R. Ma, Y.P. Wang, X.Y. Zhu, J.L. Zhang, H.C. Chan, X.F. Chen, W.J. Zhang, S.K. Chiu, G.Y. Zhu, Chem. Commun. 51 (2015) 6301–6304.
[28] R.K. Pathak, S. Marrache, J.H. Choi, T.B. Berding, S. Dhar, Angew. Chem. Int. Ed. 53 (2014) 1963–1967.
[29] R. Raveendran, J.P. Braude, E. Wexselblatt, V. Novohradsky, O. Stuchlikova,

V. Brabec, V. Gandin, D. Gibson, Chem. Sci. 7 (2016) 2381–2391.
[30] S.G. Awuah, Y.R. Zheng, P.M. Bruno, M.T. Hemann, S.J. Lippard, J. Am. Chem. Soc. 137 (2015) 14854–14857.
[31] G. Frumento, R. Rotondo, M. Tonetti, G. Damonte, U. Benatt, G.B. Ferrara, J. Exp. Med. 196 (2002) 459–468.
[32] M. Ravera, E. Gabano, G. Pelosi, F. Fregonese, S. Tinello, D. Sella, Inorg. Chem. 53 (2014) 9326–9335.
[33] A. Lopez-Flores, R. Jurado, P. Garcia-Lopez, J. Pharmacol. Toxicol. 52 (2005) 366–372.
[34] X.C. Huang, R.Z. Huang, S.H. Gou, Z.M. Wang, Z.X. Liao, H.S. Wang, Bioconjug. Chem. 28 (2017) 1305–1323.
[35] J.S. Li, Q. Han, J.M. Fang, M. Rizzi, A.A. James, J.Y. Li, Arch. Insect. Biochem. 64 (2006) 74–87.
[36] H. Lee, H. Lee, Y. Kwon, J.H. Lee, J.J. Kim, M.K. Shin, S.H. Kim, H. Bae, J. Immunol. 185 (2010) 6698–6705.
[37] X.D. Liu, N. Shin, H.K. Koblish, G.J. Yang, Q. Wang, K. Wang, L. Leffet, M.J. Hansbury, B. Thomas, M. Rupar, P. Waeltz, K.J. Bowman, P. Polam, R.B. Sparks, E.W. Yue, Y.L. Li, R. Wynn, J.S. Fridman, T.C. Burn, A.P. Combs, R.C. Newton, P.A. Scherle, Blood 115 (2010) 3520–3530.